\$ SEVIER

Contents lists available at ScienceDirect

#### Talanta

journal homepage: www.elsevier.com/locate/talanta





## Platinum nanowires/MXene nanosheets/porous carbon ternary nanocomposites for in situ monitoring of dopamine released from neuronal cells

Xueqian Xiao <sup>a,1</sup>, Wei Ni <sup>a,1</sup>, Yang Yang <sup>b</sup>, Qinhua Chen <sup>b</sup>, Yulin Zhang <sup>a,d</sup>, Yujie Sun <sup>a</sup>, Qiming Liu <sup>c</sup>, Guo-jun Zhang <sup>a,d,\*\*</sup>, Qunfeng Yao <sup>a,\*\*\*</sup>, Shaowei Chen <sup>c,\*</sup>

- <sup>a</sup> School of Laboratory Medicine, Hubei University of Chinese Medicine, Wuhan, Hubei, 430065, China
- <sup>b</sup> Shenzhen Baoan Authentic TCM Therapy Hospital, Shenzhen, Guangdong, 518101, China
- <sup>c</sup> Department of Chemistry and Biochemistry, University of California, Santa Cruz, CA, 95060, USA
- <sup>d</sup> Hubei Shizhen Laboratory, Wuhan, Hubei, 430065, China

#### ARTICLE INFO

# Keywords: Pt nanowire MXene nanosheet Composite Dopamine Electrochemical sensor PC12 cell

#### ABSTRACT

Dopamine is an important neurotransmitter in the body and closely related to many neurodegenerative diseases. Therefore, the detection of dopamine is of great significance for the diagnosis and treatment of diseases, screening of drugs and unraveling of relevant pathogenic mechanisms. However, the low concentration of dopamine in the body and the complexity of the matrix make the accurate detection of dopamine challenging. Herein, an electrochemical sensor is constructed based on ternary nanocomposites consisting of one-dimensional Pt nanowires, two-dimensional MXene nanosheets, and three-dimensional porous carbon. The Pt nanowires exhibit excellent catalytic activity due to the abundant grain boundaries and highly undercoordinated atoms; MXene nanosheets not only facilitate the growth of Pt nanowires, but also enhance the electrical conductivity and hydrophilicity; and the porous carbon helps induce significant adsorption of dopamine on the electrode surface. In electrochemical tests, the ternary nanocomposite-based sensor achieves an ultra-sensitive detection of dopamine (S/N = 3) with a low limit of detection (LOD) of 28 nM, satisfactory selectivity and excellent stability. Furthermore, the sensor can be used for the detection of dopamine in serum and in situ monitoring of dopamine release from PC12 cells. Such a highly sensitive nanocomposite sensor can be exploited for in situ monitoring of important neurotransmitters at the cellular level, which is of great significance for related drug screening and mechanistic studies.

#### 1. Introduction

Dopamine is the most abundant catecholamine neurotransmitter in the brain and plays an important role in regulating various physiological functions of the central nervous system [1]. It is synthesized by nerve cells or synapses and transmits impulses between cells to convey sensations (mainly excitement and pleasure). At the same time, it is also closely related to the body's important responses such as movement, learning, cognition, memory, and so on [2]. Abnormal dopamine concentration can create dreaded neurological diseases like Schizophrenia,

depression, Huntington's disease, Parkinson's disease, and Alzheimer's disease [3], and may trigger HIV infection [4] and the occurrence of various cancers [5]. Additionally, dopamine is a biomarker for many neurodegenerative diseases including neuroblastoma and pheochromocytoma [6]. Therefore, rapid detection and real-time quantification of dopamine in complex biofluid environments are important for evaluating neurological functions, performing relevant drug screening and studying disease mechanisms. Currently, a range of technologies have been developed for dopamine detection and analysis, such as surface-enhanced Raman spectroscopy (SERS), fluorescence,

<sup>\*</sup> Corresponding author.

<sup>\*\*</sup> Corresponding author. School of Laboratory Medicine, Hubei University of Chinese Medicine, Wuhan, Hubei, 430065, China.

<sup>\*\*\*</sup> Corresponding author.

E-mail addresses: zhanggi@hbtcm.edu.cn (G.-j. Zhang), yaoqunfeng@hbtcm.edu.cn (Q. Yao), shaowei@ucsc.edu (S. Chen).

These authors contributed equally to this work.

spectrophotometry, gas chromatography-mass spectrometry, and so on [7]. These methods often require sophisticated instrumentation and delicate operations, are time-consuming, and greatly limits their application in clinical testing. The detection can be further complicated by the fact that dopamine can be easily polymerized or oxidized [8]. In addition, the content of dopamine in the human body is very low (e.g.,  $0.01-1~\mu M$  in healthy individuals, and in the nanomolar range in patients with Parkinson's disease) [9], and there are interferences from substances such as uric acid (UA) and ascorbic acid (AA), which makes the accurate detection of dopamine even more difficult. Therefore, there is an urgent need for the rational design and development of sensitive, selective, rapid, and inexpensive dopamine assays.

Towards this end, electrochemistry stands out as an attractive option due to the ease of operation, simple instrumentation, no complex pretreatment, and low cost [10]. However, bare electrodes typically exhibit only low electron-transfer kinetics and are prone to interference by non-specific substances, which greatly compromises the detection sensitivity. The performance can be improved by modifying the electrode surface with active materials [11], such as magnetic nanoparticles [12], carbon nanotubes [13], metal nanoparticles [14], carbon quantum dots [15], as well as graphene [16]. For example, Huang et al. [17] prepared an ultra-sensitive electrochemical sensor for dopamine detection based on graphene quantum dots/multi-walled carbon nanotubes (GQDs-MWCNTs), whereby the GQDs significantly increased the specific surface area and improved the electrical conductivity of the electrode. Ma et al. [18] developed an electrochemical sensor based on self-rolled TiO2 microscroll/graphene composites, where the sensitivity and selectivity for dopamine detection was significantly enhanced, due to the porous surface of the TiO<sub>2</sub> nanomembranes and highly conductive graphene. Other 2D nanomaterials, such as transition metal dichalcogenides and MoS<sub>2</sub> [19], have also been used for electrochemical bioassays. Among these, MXenes [20] have emerged as a unique option, due to good hydrophilicity and excellent mechanical properties, with rich surface functional groups, such as -OH, -O, and -F [21]. Few-layer or monolayer MXenes nanosheets are known to possess a large specific surface area and adjustable interlayer gap, which not only effectively improve the electrical conductivity but also reduce the aggregation and accumulation of atoms [22]. Therefore, MXenes can be used as an ideal support for loading other substances [23]. Since Zheng' group experimentally demonstrated dopamine detection by MXenes in 2018, MXenes have been widely used for the electrochemical detection of dopamine and other biomolecules [24]. The performance can be further enhanced by the incorporation of three-dimensional porous carbon (PC) that is known to markedly enhance the adsorption capacity and electron/mass transfer kinetics [25].

Metal nanoparticles/nanostructures represent another class of active materials due to their unique catalytic activity. He et al. [26] loaded gold nanoparticles onto a graphene film and observed highly sensitive and rapid detection of dopamine under optimal conditions. Sun et al. [27] prepared a dopamine sensor based on BiOI and AuAg nanoparticles modified indium tin oxide (ITO) electrodes, where the AuAg nanoparticles improved the surface conductivity of BiOI and significantly increased the sensitivity and stability of the sensor. Platinum (Pt) is another metal with excellent catalytic activity [28]. Yet, Pt-based catalysts are mostly concentrated on Pt nanoparticles, which exhibit a high surface energy, and are prone to dissolution, aggregation, and/or Oswald ripening during catalytic reactions [29]. Such issues may be mitigated with one-dimensional (1D) Pt nanostructures, such as nanowires (NWs) and nanotubes (NTs) [30], which feature unique structural characteristics such as good flexibility, stable configuration, and numerous high-coordination atoms. In particular, the rich grain boundaries of Pt nanowires are favorable for enhancing the catalytic activity by lowering the reaction activation energy [31].

In this study, ternary nanocomposites consisting of Pt nanowires/ MXene nanosheets/porous carbon (Pt/MX/PC) were prepared and used as the active materials to construct a sensing platform for dopamine detection based on screen printed carbon electrodes (SPCEs) (Scheme 1). Ti<sub>3</sub>C<sub>2</sub>T<sub>x</sub> MXene nanosheets were prepared by chemical etching with HCl and LiF and uniformly dispersed in an organic solvent under sonication. Subsequently, H<sub>2</sub>PtCl<sub>6</sub> and KOH were co-incubated at high temperature and pressure, where Pt atoms were anchored onto the surface of the MXene nanosheets through amine species produced in the system, which promoted the growth of Pt nanowires. Finally, porous carbon was added to the Pt nanowires/MXene suspension, and the resulting Pt/MX/PC ternary nanocomposites were dropcast onto the SPCE surfaces for electrochemical detection of dopamine. Within the ternary nanocomposite, the MXene nanosheets loaded with Pt nanowires possessed abundant active sites, the Pt nanowires inhibited the interlayer aggregation of the MXene nanosheets and increased the surface area for improved catalytic activity, while PC enhanced the adsorption of dopamine on the electrode surface, and the porous mesh structure also increased the specific surface area and facilitated charge and mass transfer. The synergistic effects of these structural components led to a remarkable performance in dopamine detection.

#### 2. Experimental section

#### 2.1. Materials

 $Ti_3AlC_2$  MAX (>95 % purity) was purchased from Beike 2D materials Co. Ltd. Hexachloroplatinic acid ( $H_2PtCl_6\cdot 6H_2O$ , >99 % purity) was purchased from Aladdin Co. Ltd. Potassium citrate was purchased from Alfa Aesar. All other reagents were of analytical grade and used as supplied. SPCEs were obtained from Zhejiang Nazhihui Biotechnology Co

#### 2.2. Synthesis and characterization of Pt/MX/PC nanocomposites

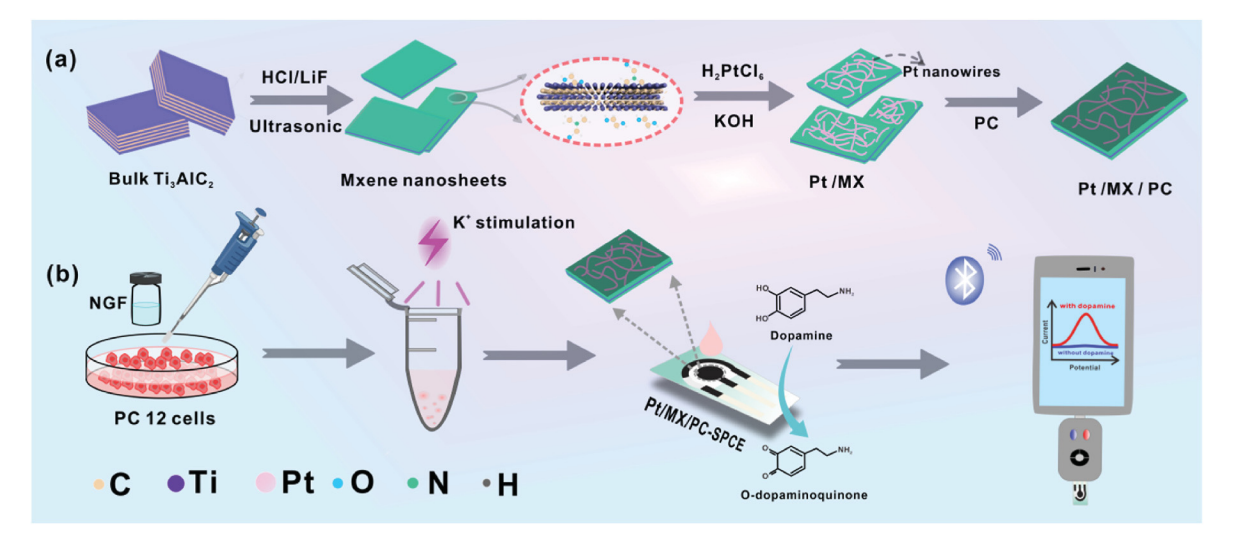
 $Ti_3C_2Tx$  MXene nanosheets were fabricated by traditional acid etching with HCl and LiF from bulk  $Ti_3AlC_2$  (MAX), and 60 mg was dispersed in 15 mL of ethylene glycol and 20 mL of N,N-dimethylformamide (DMF) under sonication for 2 h to obtain a black suspension. Into this was then added 40 mg of  $H_2PtCl_6$  and 2 g of KOH under vigorous stirring overnight, before the mixture was transferred to a Teflon autoclave and solvothermally treated at 170 °C for 8 h. In this process, Pt was anchored onto the surface of the  $Ti_3C_2Tx$  MXene nanosheets through the amine species produced in the system, leading to the growth of abundant Pt nanowires assembled onto the MXene nanosheets. After the reaction, the product was cooled to room temperature, collected by centrifugation, rinsed with ethanol and ultrapure water for several times, and finally freeze-dried, affording Pt nanowires/MXene nanosheets (Pt/MX) binary composites.

PC was synthesized by adopting a procedure reported previously [32]. In brief, 8 mmol of potassium citrate (Alfa Aesar Co., Ltd.) was placed in a tube furnace and pyrolyzed at 800 °C for 1 h in an Ar atmosphere. The resulting black solid was rinsed with a  $\rm H_2SO_4$  solution (0.5 M) and water (18.2 M $\Omega$ ) to remove inorganic impurities, and dried at 60 °C, to yield PC.

The obtained PC was mixed with the above Pt/MX at a 1:1 mass ratio to produce ternary Pt/MX/PC nanocomposites. The structural characterization was conducted with a field-emission transmission electron microscope (TEM, FEI Talos F200S), scanning electron microscope (SEM, Hitachi S-4800), PHI Quantera X-ray electron spectroscopy (XPS) instrument, a Rigaku Ultima IV X-ray diffractometer ( $\lambda=0.15418$  nm), and PerkinElmer Spectrum One FTIR spectrometer. Dynamic light scattering (DLS) and zeta potential studies were carried out by using a Wyatt DynaPro NanoStar temperature-controlled microsampler.

#### 2.3. Preparation of Pt/MX/PC sensors

SPCEs were used as the biosensor platform, where three electrodes were printed with an external insulating layer and electrode leads,



Scheme 1. Schematic illustrations of (a) the synthetic process of Pt nanowires/MXene nanosheets/porous carbon (Pt/MX/PC) ternary nanocomposites, and (b) the detection of dopamine released from living PC12 cells.

namely, the working electrode (WE), the reference electrode (RE), and the auxiliary electrode (AE). To prepare the catalyst ink, 1 mg of the Pt/MX/PC ternary composites were dispersed into 1 mL of a 10 % Nafion solution under sonication for 30 s and 10  $\mu L$  of the ink was dropcast onto the WE and allowed to dry at room temperature in a dustless environment. The resulting SPCEs were then used for electrochemical detection of dopamine.

#### 2.4. Electrochemistry

All electrochemical tests were run with a CHI 660E electrochemical workstation (Shanghai CH Instrument, China) with the SPCEs at room temperature. In real serum tests, the samples were diluted with  $1\times$  PBS (phosphate buffer saline, pH 7.4) to obtain 5 % serum, into which was added dopamine at different known concentrations. The recovery of the samples was calculated from the current signals.

#### 2.5. PC12 cells culture and dopamine detection

A PC12 cell line was cultivated and maintained in a cell culture flask using a Roswell Park Memorial Institute (RPMI) Medium 1640 supplemented with 5 % heat-inactivated fetal bovine serum (FBS), 15 % heatinactivated horse serum (HS), and 1 % penicillin-streptomycin at 37 °C, placed in a humidified atmosphere of 95 % air and 5 % carbon dioxide. Cells were passaged every 4–5 d and the medium was changed 3–4 times a week throughout the lifetime of all cultures. Cells were trypsinized and subcultured when they grew to more than 80 % confluence in the Tflask. All culture flasks used were washed with 0.01 % poly-L-lysine solution for 2 h before inoculation, followed by fresh RPMI 1640 medium (or  $1 \times PBS$ ). Nerve growth factor (NGF) was added to the culture flasks at a concentration of 50 ng/mL and incubated for 48 h prior to the electrochemical experiments [33]. Then, PC12 cells were removed from the bottom of the cell culture flasks by standard trypsinization, and the cell density was determined to be approximately  $1 \times 10^5$  cells/mL by cell counting method, followed by resuspension in PBS after centrifugation. A high K<sup>+</sup> solution was then added to the reaction system to depolarize the living PC12 cells and induce dopamine release. After co-incubation for 6 min, voltammetric measurements and mass spectrometry analysis (Instrument: AB SCIEX 6500+ Mass Spectrometer) were performed to detect dopamine.

#### 3. Results and discussion

#### 3.1. Characterization of Pt/MX/PC ternary composites

The morphology and microstructure of the Pt/MX/PC composites were first analyzed using SEM and TEM measurements. From the SEM image in Fig. 1a, the sheet morphology of the MXene layers can be clearly observed. From the TEM (Fig. 1b) and SEM (Fig. S1a) images of the Pt/MX composites, the Pt nanowires (along with a small number of nanoparticles) can be found to be dispersed on the MXene surface forming an integrated network. In high-resolution transmission electron microscopy (HRTEM) measurements of the Pt/MX composites (Fig. 1c), the Pt nanowires can be seen to possess well-defined lattice fringes with an interplanar spacing of 0.235 nm consistent with the (111) planes of cubic platinum [34], and rich grain boundaries (yellow dashed lines). Fig. S1b shows the SEM image of PC, which can be seen to contain a number of pores of varying sizes (from a few tens to a few hundred nm), forming an integrated network structure. Fig. 1d shows a SEM image of the Pt/MX/PC ternary composites. A clear three-dimensional porous structure can be observed due to the coverage of the Pt/MX surface by PC with excellent adsorption property. Fig. 1e shows the high-angle annular dark-field scanning TEM (HAADF-STEM) image of the Pt/MX/PC ternary nanocomposites, where the Pt nanowires/nanoparticles can be readily resolved. In fact, in elemental mapping analysis based on energy-dispersive X-ray spectroscopy (Fig. 1f-i), the elements of Pt, O, C and Ti can be clearly identified, where Pt can be seen to be confined within the nanowires/nanoparticles, whereas the others were homogeneously distributed across the entire sample.

XPS study was then carried out to examine the elemental composition and chemical valence of the samples. From the survey spectrum of the Pt/MX sample in Fig. 2a, the C 1 s, Ti 2p, O 1s and Pt 4f electrons can be readily resolved at 284, 458, 530, and 71 eV, respectively (the F 1s and K 2p electrons can also be observed at 687 and 378 eV, due to residual precursors). For PC, only the characteristic peaks of C 1s and O 1s are visible at 284 and 530 eV, respectively. All these peaks can be clearly resolved in the Pt/MX/PC ternary composite which was prepared by mixing Pt/MX and PC at a 1:1 mass ratio. The high-resolution scan of the O 1s electrons of Pt/MX/PC is shown in Fig. 2b, where deconvolution yields four subpeaks at 529.6, 531.0, 531.8, and 532.8 eV, corresponding to the O-metal, O=C, OH-metal, and O=F groups, respectively [35]. The corresponding Pt 4f spectrum (Fig. 2c) can be seen to consist of two  $(4f_{7/2}/4f_{5/2})$  doublets, metallic Pt at 70.1/73.5 eV and Pt (II) at 75.3/71.4 eV [36], confirming that most Pt of the precursors was

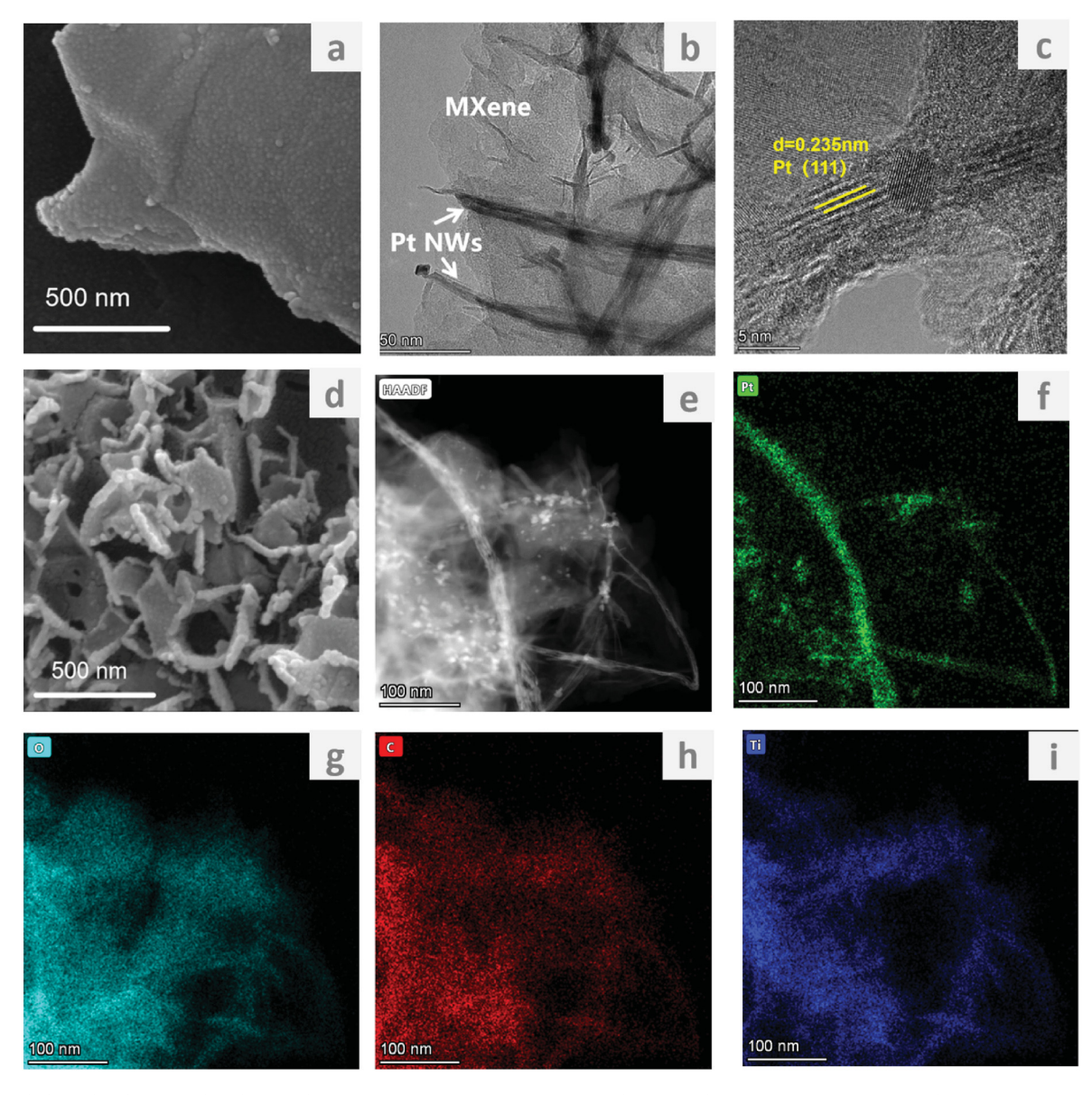


Fig. 1. Morphological and structural analyses of the Pt/MX/PC. (a) SEM image of MXene. (b) TEM and (c) HRTEM images of Pt/MX binary composites. (d) SEM and (e) HAADF-STEM images of Pt/MX/PC ternary composites and the corresponding elemental maps of (f) Pt, (g) O, (h) C, and (i) Ti.

solvothermally reduced to metallic Pt in ethylene glycol. It is noteworthy that the Pt 4f binding energy of Pt/MX/PC was shifted negatively by approximately 0.8 eV in comparison with those of conventional Pt/C [37]. Such electron enrichment most likely arose from strong electronic interactions between the Pt nanowires and  $Ti_3C_2Tx$ . Fig. 2d depicts the Ti 2p spectrum, which contained three  $(2p_{3/2}/2p_{1/2})$  doublets, C–Ti-Tx  $(456.9/462.7 \, \text{eV})$ ,  $TiO_2$   $(457.7/463.6 \, \text{eV})$ , and Ti-O-X  $(458.3/464.4 \, \text{eV})$  [38]. The formation of  $TiO_2$  was likely due to surface oxidation of  $Ti_3C_2T_x$  nanosheets during the solvothermal synthesis. Three species were resolved from the C 1s scan (Fig 2e), C–C  $(284.9 \, \text{eV})$ , C–O  $(286 \, \text{eV})$  and C—O  $(287.6 \, \text{eV})$  [39].

The X-ray diffraction (XRD) patterns are shown in Fig. 2f. One can see that PC possessed a broad diffraction peak centered at  $2\theta \approx 25^\circ$  and a minor one at ca.  $44^\circ$  corresponding to the (002) and (100) crystalline facets of graphitic carbon (the series of sharp peaks were likely due to the aluminum substrate in XRD measurements) [40]. For Pt/MX, the characteristic diffraction peaks of MXenes can be found at ca.  $19^\circ$ ,  $42^\circ$ , and  $55^\circ$  for the (002), (210) and (211) crystalline facets, respectively [41]; whereas the diffraction patterns at  $2\theta \approx 38^\circ$ ,  $47^\circ$ ,  $68^\circ$  and  $82^\circ$  can be indexed to the (111), (200), (220) and (311) crystal planes of

face-centered-cubic Pt, respectively [42] (the weak peaks at  $45^\circ$  and  $55^\circ$  can be assigned to the (210) and (211) crystal facets of  $\text{TiO}_2$ , which was likely produced by the unavoidable surface oxidation of  $\text{Ti}_3\text{C}_2\text{T}_x$  during the solvothermal process [43]). All these diffraction features can be resolved with Pt/MX/PC, which possessed an additional diffraction peak at ca.  $60^\circ$ , corresponding to the (110) facets of the  $\text{Ti}_3\text{C}_2\text{Tx}$  nanosheets [44]. This observation confirmed the successful production of the ternary composite.

Consistent results were obtained from the FITR measurements. From Fig. 2g, a series of vibrational features can be resolved for the sample series, O–H stretch at 3428 cm $^{-1}$ , C=O stretch at 1630 cm $^{-1}$ , Ti–O vibration at 950 cm $^{-1}$  and Ti–C vibration at 590 cm $^{-1}$ . In DLS measurements (Fig. 2h), the average hydrodynamic radius of Pt/MX/PC can be seen to be markedly larger than those of PC and Pt/MX, and the Zeta potential ( $\zeta$ ) of Pt/MX/PC (-26 mV) can be found to be in the intermediate between those of PC(-22.9 mV) and Pt/MX (-28 mV) (Fig. S2). Taken together, these results further confirmed the successful production of ternary Pt/MX/PC composites.

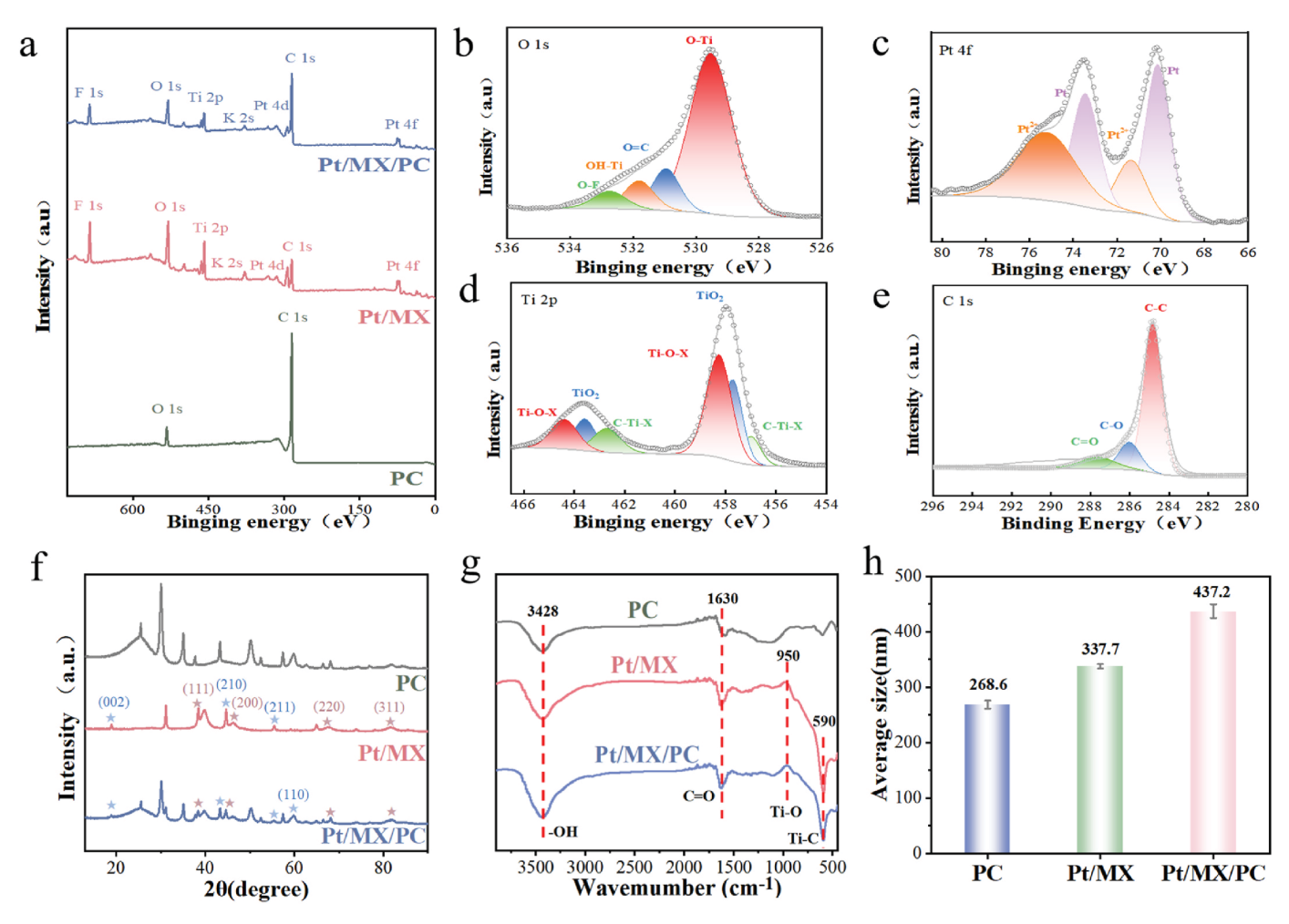


Fig. 2. Structural characterizations of the Pt/MX/PC ternary composites. (a) XPS survey spectra of Pt/MX, PC, and Pt/MX/PC. High-resolution scans of the (b) O 1s, (c) Pt 4f, (d) Ti 2p and (e) C 1s electrons of Pt/MX/PC. (f) XRD patterns, (g) FTIR spectra, and (h) average size of PC, Pt/MX and Pt/MX/PC.

#### 3.2. Dopamine detection by Pt/MC/PC-modified SPCE

The electrochemical activity of the Pt/MC/PC-modified SPCE was first tested in a  $[Fe(CN)_6]^{3-/4}$ - solution. From the cyclic voltammograms in Fig. 3a, a pair of voltametric peaks with a formal potential (E°') of +0.127 V can be clearly seen at bare SPCE, Pt/MX-modified SPCE and Pt/MX/PC-modified SPCE, with the peak current (I<sub>p</sub>) increasing in the

order of bare SPCE < Pt/MX-modified SPCE < Pt/MX/PC-modified SPCE, most likely due to enhanced electrochemically active surface area arising from the three-dimensional PC scaffold (Fig. S1b). Fig. 3b depicts the corresponding Nyquist plots at the open-circuit potential (+0.19 V), where the charge-transfer resistance ( $R_{ct}$ ) [45] can be seen to diminish in the order of bare SPCE ( $1032~\Omega$ ) > Pt/MX-modified SPCE ( $856~\Omega$ ) > Pt/MX/PC-modified SPCE ( $856~\Omega$ ) suggesting enhanced

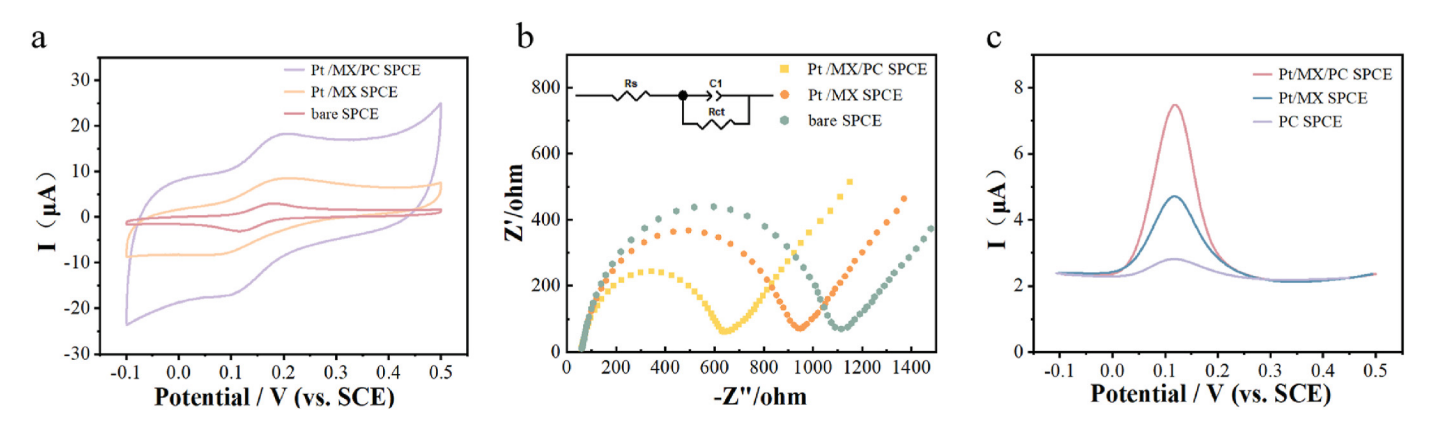


Fig. 3. (a) CV curves in 5 mM Fe(CN) $_6^{3-/4-}$  solution at bare SPCE, Pt/MX-modified SPCE and Pt/MX/PC-modified SPCE. Scan rate: 100 mV/s. (b) Nyquist plots at open circuit potential in 5 mM Fe(CN) $_6^{3-/4-}$  solution at bare SPCE, Pt/MX-modified SPCE and Pt/MX/PC-modified SPCE. Frequency range from 0.01 Hz to 100 kHz. AC amplitude 5 mV. Inset is the equivalent circuit, where  $R_{ct}$  is charge-transfer resistance,  $C_1$  is double-layer capacitance, and  $R_s$  is serial resistance. (c) DPV measurements of PC SPCE, Pt/MX SPCE and Pt/MX/PC SPCE after electrodeposition at 0 V for 60 s in 1 × PBS containing 100  $\mu$ M DA.

electron-transfer kinetics most likely due to the rich grain boundaries of the Pt nanowires and the excellent electrical conductivity of PC.

We then examined the performance of the modified electrode towards dopamine detection. From Fig. 3c, one can see that after electrodeposition at 0 V for 60 s in 100  $\mu M$  dopamine, all PC-, Pt/MX- and Pt/MX/PC-modified SPCEs exhibited an oxidation peak at +0.12 V in differential pulse voltammetry (DPV) measurements, and the peak current increased in the order of PC-modified SPCE < Pt/MX-modified SPCE < Pt/MX/PC-modified SPCE, suggesting the unique potential of the Pt/MX/PC ternary composites in dopamine detection. Note that 60 s was the optimal electrodeposition time, as the DPV peak current mostly levelled off at prolonged electrodeposition (Fig. S3). In addition, to identify the optimal pH, cyclic voltammograms (CVs) were collected with the Pt/MX/PC-modified SPCE in 100  $\mu M$  dopamine with the solution pH varied from 4 to 9 (Fig. 4a), and the voltametric peak current can be seen to reach the maximum at pH = 7 (Fig. 4b, blue curve), which was therefore identified as the optimal pH. Also, one can see a good linear relationship between the oxidation peak potential and pH, E<sub>p</sub> (V) =  $-0.0614 \text{ pH} + 0.6980 \text{ (R}^2 = 0.991, \text{ red curve in Fig. 4b), where the slope}$ of -0.0614 V/pH is close to the theoretical value (-59.2 mV/pH) [46], suggesting participation of an equal number protons and electrons in the overall redox reaction.

Fig. S4a shows the CVs of the Pt/MX/PC-modified SPCE in  $1\times$  PBS solution (pH = 7.4) containing 100  $\mu\text{M}$  of dopamine at different potential scan rates (from 10 to 200 mV/s). One can see a good linear relationship between the peak current (Ip) and scan rate (Fig. S4b), suggesting that the current signals were from surface-adsorbed dopamine [47]. DPV measurements were then carried out with the addition of dopamine at different concentrations in PBS (pH = 7.4) (Fig. 4c), where one can see that the peak current (Ip) increased linearly with the dopamine concentration (C) within the wide concentration range of 0.1–200  $\mu\text{M}$  (Fig. 4d), Ip ( $\mu\text{A}$ ) = 3.012 + 0.051C ( $\mu\text{M}$ ) (R $^2$  = 0.991), with a limit of detection (LOD; S/N = 3) of 28 nM. Such a performance was highly comparable to leading results reported in the literature with relevant electrochemical sensors (Table 1).

Table 1
Performance comparison for dopamine detection between the Pt/MX/PC-modified SPCE and other relevant sensors in the literature.

Electrode Material	Methods	Linear Range	Low Detection Limit	references
Ti <sub>3</sub> C <sub>2</sub> T <sub>x</sub> (MXene)/Au NPs	DPV	2.0–500.0 μΜ	0.670 μΜ	[47]
IL (1-methyl imidazolium acetate)/MXene (Ti <sub>3</sub> C <sub>2</sub> Cl <sub>2</sub> )/GPE	DPV	10.0–2000.0 μM	0.702 μΜ	[48]
MOF-MXene(Ti <sub>3</sub> C <sub>2</sub> )	DPV	90.0-300.0 nM	0.110 μΜ	[49]
Nb <sub>2</sub> C MXene/ZnS	DPV	0.09-0.82 mM	1.390 μΜ	[50]
NS-Nb <sub>2</sub> C MXene	DPV	0.4-90.0 μΜ	0.120 μΜ	[51]
Perylene diimide/ MXene	DPV	100.0–1000.0 μΜ	0.240 μΜ	[52]
Au-Pd/MXene	DPV	12.0-240.0 μM	0.130 μΜ	[53]
Pt NWs/MXene/ porous carbon	DPV	0.1–200.0 μΜ	0.028 μΜ	This work

### 3.3. Selectivity, reproducibility, and stability of Pt/MX/PC SPCE for dopamine detection

To examine the practical reliability of the Pt/MX/PC-modified SPCE electrochemical sensing platform, the performance was evaluated within the context of selectivity, reproducibility, and stability. DPV measurements were carried out in a PBS solution (pH = 7.4) where a series of interferents, which are commonly found with dopamine in the real organism environment, such as uric acid (UA), ascorbic acid (AA), glucose, citric acid, urea and various amino acids, were added separately into the reaction system. The current response at  $+0.12\,V$  was plotted in Fig. 5a. One can see a significant current signal upon the addition of 100  $\mu$ M of dopamine, while no obvious current response was observed with the addition of these interferents even at 10 times excess [42]. This indicates good selectivity of the electrochemical sensor for dopamine and great potential for practical applications, likely due to the unique affinity of the amine moiety of dopamine to the Pt surface.

Subsequently, the reproducibility and stability of Pt/MX/PC-based

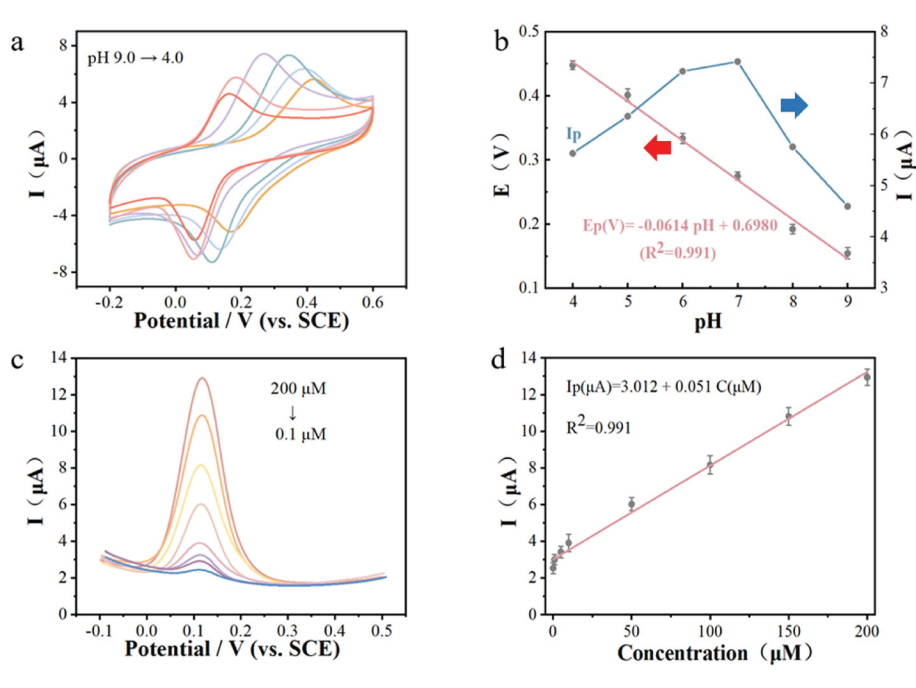


Fig. 4. (a) Cyclic voltammograms of Pt/MX/PC-modified SPCE in 100  $\mu$ M dopamine at different pH (from 4 to 9). Scan rate 10 mV/s. (b) Effect of pH on peak currents (blue curve) and the linear relationship between peak potential and pH (red curve). (c) DPV profiles of dopamine at different concentrations (200, 150, 100, 50, 10, 50, 10, 51, and 0.1  $\mu$ M) in 1  $\times$  PBS (pH 7.4) at the Pt/MX/PC-modified SPCE, and (d) the corresponding linear curve of DPV peak current and dopamine.

Fig. 5. (a) DPV peak current of 100  $\mu$ M DA and 1 mM UA, AA, glucose, citric acid, urea, cysteine, lysine, glycine at Pt/MX/PC-modified SPCE in 1  $\times$  PBS (pH = 7.4). (b) DPV peak currents of five Pt/MX/PC-modified SPCEs prepared independently in a 1  $\times$  PBS solution containing 100  $\mu$ M DA. (c) DPV peak currents of Pt/MX/PC-modified SPCE in 1  $\times$  PBS solution containing 100  $\mu$ M DA in 7 days.

sensors were investigated in PBS solution (pH = 7.4). The DPV profiles of five electrodes fabricated separately were recorded in the presence of 100  $\mu$ M dopamine under the same conditions, and each electrode was repeated 3 times to evaluate the reproducibility. The difference of the current signals between the 5 electrodes did not exceed 3 %, and the relative standard deviation (RSD) of the three repeated tests was within 5 % (Fig. 5b), indicating satisfactory reproducibility and stability. Finally, the stability was also assessed by evaluating the ratio of the current signal to the initial value for 7 d, which showed a retention rate over 95 % (Fig. 5c).

To further test the accuracy of the prepared dopamine electrochemical sensor, recovery tests were performed in serum by standard addition method. Dopamine was added to a 20-fold dilution of serum under optimal reaction conditions. The measured amount and recovery rate were calculated according to the linear equation, and the samples were measured three times in parallel. The results are shown in Table 2. The recovery of the samples was between 92.30 % and 95.80 %, indicating that the modified electrode can be applied to the determination of actual samples.

#### 3.4. Detection of dopamine released from live PC12 cells

Notably, the Pt/MX/PC-modified SPCE also demonstrated a remarkable performance towards the detection of dopamine generated in situ by live PC12 cells. It is known that stimulation of highconcentration K<sup>+</sup> promotes depolarization of PC12 cells and induces the release of dopamine [54]. Experimentally, we cultured PC12 neural cells and recorded changes in cell growth morphology. As shown in Fig. 6a and b, without the addition of NGF that stimulates cell differentiation, the PC12 cells exhibited a spherical morphology and tended to grow in clusters. After the addition of NGF, the cells became pike-shaped and polygonal, and grew elongated synapses step by step, a typical morphological feature of nerve cells [33]. This indicated that the PC12 cells were successfully cultured. Then, we explored the biosafety of Pt/MX/PC by CCK8 assays. As shown in Fig. 6c, upon the co-incubation of the ternary composites at a high (5  $\mu$ g/mL) or low (1  $\mu$ g/mL) concentrations with live PC12 cells for 8, 16 and 24 h, the cellular activity remained above 85 %, indicating that the material had no obvious

**Table 2** Recovery measurements of dopamine in serum by the Pt/MX/PC-modified SPCE (n = 3).

Sample	Added (µm)	Found (µm)	Recovery (%)	RSD (%)
1	1.0	0.923	92.30	4.29
2	10.0	9.490	94.90	4.58
3	100.0	95.810	95.80	3.65

killing of the cells, which confirmed good biocompatibility.

PC12 cells will gradually release dopamine under high-concentration  $K^+$  stimulation, and an increasing amount of dopamine will be accumulated in the solution with time. Three different concentrations of  $K^+$  ions were chosen (30, 20, and 10 mM, corresponding to curves A, B, and C, respectively, in Fig. 6d). After 6 min of incubation, the amount of dopamine in the solution was detected by DPV measurements, where the higher the  $K^+$  concentration, the stronger the current signals, in contrast to the control groups (Fig. 6d, E and F curves) which exhibited a largely featureless response. Remarkably, the dopamine contents obtained from the Pt/MX/PC-modified SPCE were consistent with those from mass spectrometry measurements (Fig. S5), which suggests high potential of the electrochemical sensor for clinical application.

The excellent performance of the Pt/MX/PC-based sensor can be ascribed to the unique ternary composite structure. The sensor was able to detect dopamine sensitively and rapidly even at low concentrations. This is of particular significance due to the low content of dopamine in the body. In addition, the excellent selectivity to dopamine makes it free from the interference of other substances in the complex body fluids. Successful real-time monitoring of dopamine in PC12 cells opens up a new way for in situ monitoring of neurotransmitters in nerve cells. Such unique properties can be exploited for the development of new effective technologies for drug screening and mechanistic studies.

#### 4. Conclusions

In this work, an electrochemical biosensing platform was constructed based on Pt/MX/PC ternary nanocomposites for highly sensitive and rapid detection of dopamine, which featured a low detection limit of 28 nM and a linear range of 0.1–200  $\mu M$ , as well as excellent selectivity, reproducibility and stability. Importantly, the Pt/MX/PC-based biosensor could also be used to detect dopamine released from living cells after treatment with stimulants, as manifested in situ monitoring of dopamine released from PC12 cells. Results from the work highlight the unique potential of Pt/MX/PC ternary nanocomposites as active materials for the rapid and accurate detection of biomarkers.

#### CRediT authorship contribution statement

Xueqian Xiao: Writing – original draft, Formal analysis, Data curation. Wei Ni: Writing – original draft, Formal analysis, Data curation. Yang Yang: Formal analysis, Data curation. Qinhua Chen: Formal analysis, Data curation. Yulin Zhang: Writing – original draft, Funding acquisition, Formal analysis. Yujie Sun: Data curation. Qiming Liu: Formal analysis. Guo-jun Zhang: Writing – original draft, Project administration, Funding acquisition, Formal analysis,

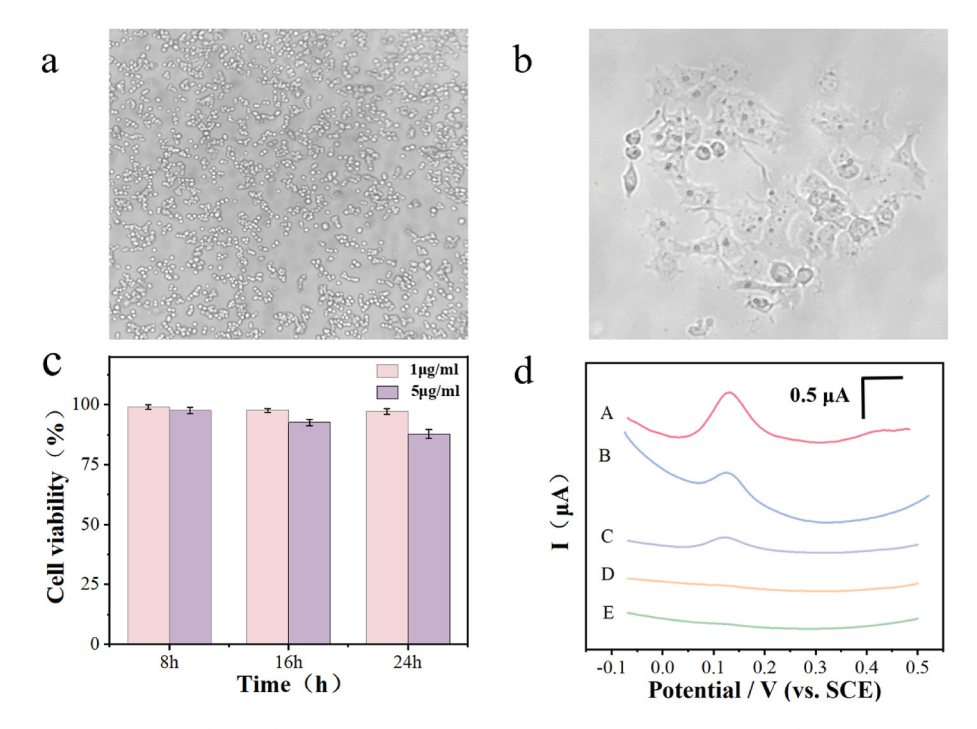


Fig. 6. Morphological observations in PC 12 cells (a) cultured for 2 d without NGF and (b) cultured for 5 d after the addition of NGF. (c) Cell viability tests of the Pt/MX/PC SPCE after co-culturing with PC 12 cells for 8, 16, and 24 h, respectively. (d) DPV responses of the Pt/MX/PC SPCE in high K<sup>+</sup> solution with cultured PC 12 cells in the presence of (A) 30, (B) 20, and (C) 10 mM K<sup>+</sup>, and (D) K<sup>+</sup> solution without PC 12 cells, and (E) PC 12 cells solution only without K<sup>+</sup>.

Conceptualization. **Qunfeng Yao:** Writing – original draft, Project administration, Funding acquisition, Formal analysis, Conceptualization. **Shaowei Chen:** Writing – review & editing, Project administration, Funding acquisition, Formal analysis, Conceptualization.

#### Declaration of competing interest

The authors declare that they have no known competing financial interests or personal relationships that could have appeared to influence the work reported in this paper.

#### Data availability

Data will be made available on request.

#### Acknowledgments

This work was funded with the support from the Natural Science Fund of Hubei Province (No.2023AFD157). Dr Qinhua Chen is thankful for the support from Sanming Project of Medicine in Shenzhen (No. SZZYSM202106004) and the National Natural Science Foundation of China (82272960). G.-J.Z. is grateful to the support from the National Key Research and Development Program of China (2022YFB3204403) and Hubei Province Centralized Guided Local Science and Technology Development Special Project (2022BGE271).

#### Appendix A. Supplementary data

Supplementary data to this article can be found online at https://doi.org/10.1016/j.talanta.2024.126496.

#### References

- T. Panapimonlawat, S. Phanichphant, S. Sriwichai, Electrochemical dopamine biosensor based on poly(3-aminobenzylamine) layer-by-layer self-assembled multilayer thin film, Polymers 13 (2021) 1488.
- [2] J.D. Berke, What does dopamine mean? Nat. Neurosci. 21 (2018) 787-793.

- [3] A.P.F. Chen, L. Chen, T.A. Kim, Q. Xiong, Integrating the roles of midbrain dopamine circuits in behavior and nNeuropsychiatric disease, Biomedicines 9 (2021) 647.
- [4] P.J. Gaskill, D.R. Miller, J. Gamble-George, H. Yano, H. Khoshbouei, HIV, Tat and dopamine transmission, Neurobiol. Dis. 105 (2017) 51–73.
- [5] P. Sobczuk, M. Lomiak, A. Cudnoch-Jedrzejewska, Dopamine D1 receptor in cancer, Cancers 12 (2020) 3232.
- [6] J. Garcia-Pardo, F. Novio, F. Nador, I. Cavaliere, S. Suarez-Garcia, S. Lope-Piedrafita, A.P. Candiota, J. Romero-Gimenez, B. Rodriguez-Galvan, J. Bove, M. Vila, J. Lorenzo, D. Ruiz-Molina, Bioinspired theranostic coordination polymer nanoparticles for intranasal dopamine replacement in Parkinson's disease, ACS Nano 15 (2021) 8592–8609.
- [7] H.K. Choi, J.H. Choi, J. Yoon, An updated review on electrochemical nanobiosensors for neurotransmitter detection, Biosensors 13 (2023) 892.
- [8] X. Liu, J. Liu, Biosensors and sensors for dopamine detection, View 2 (2020) 20200102.
- [9] S. Lakard, I.-A. Pavel, B. Lakard, Electrochemical biosensing of dopamine neurotransmitter: a review, Biosensors 11 (2021) 179.
- [10] M. Labib, E.H. Sargent, S.O. Kelley, Electrochemical methods for the analysis of clinically relevant biomolecules, Chem Rev 116 (2016) 9001–9090.
- [11] A. Chen, S. Chatterjee, Nanomaterials based electrochemical sensors for biomedical applications, Chem. Soc. Rev. 42 (2013) 5425–5438.
- [12] A. Thamilselvan, P. Manivel, V. Rajagopal, N. Nesakumar, V. Suryanarayanan, Improved electrocatalytic activity of Au@Fe(3)O(4) magnetic nanoparticles for sensitive dopamine detection, Colloids Surf. B Biointerfaces 180 (2019) 1–8.
- [13] Y. Yang, M. Li, Z. Zhu, A novel electrochemical sensor based on carbon nanotubes array for selective detection of dopamine or uric acid, Talanta 201 (2019) 295–300.
- [14] J. Tang, Y. Liu, J. Hu, S. Zheng, X. Wang, H. Zhou, B. Jin, Co-based metal-organic framework nanopinnas composite doped with Ag nanoparticles: a sensitive electrochemical sensing platform for simultaneous determination of dopamine and acetaminophen, Microchem. J. 155 (2020) 104759.
- [15] S. Paulo-Mirasol, C. Izquierdo, C. Alemán, E. Armelin, J. Torras, Flexible electrode based on nitrogen carbon quantum dots for dopamine detection, Appl. Surf. Sci. 626 (2023) 157241.
- [16] Y.R. Kim, S. Bong, Y.J. Kang, Y. Yang, R.K. Mahajan, J.S. Kim, H. Kim, Electrochemical detection of dopamine in the presence of ascorbic acid using graphene modified electrodes, Biosens. Bioelectron. 25 (2010) 2366–2369.
- [17] Q. Huang, X. Lin, L. Tong, Q.-X. Tong, Graphene quantum dots/multiwalled carbon nanotubes composite-based electrochemical sensor for detecting dopamine release from living cells, ACS Sustain. Chem. Eng. 8 (2020) 1644–1650.
- [18] F. Ma, B. Yang, Z. Zhang, J. Kong, G. Huang, Y. Mei, Self-rolled TiO2 microscroll/graphene composite for electrochemical dopamine sensing, Prog. Nat. Sci.: Mater. Int. 30 (2020) 337–342.
- [19] L. Wang, Q. Xiong, F. Xiao, H. Duan, 2D nanomaterials based electrochemical biosensors for cancer diagnosis, Biosens. Bioelectron. 89 (2017) 136–151.

[20] M. Naguib, M. Kurtoglu, V. Presser, J. Lu, J. Niu, M. Heon, L. Hultman, Y. Gogotsi, M.W. Barsoum, Two-dimensional nanocrystals produced by exfoliation of Ti3 AlC2, Adv Mater 23 (2011) 4248–4253.

- [21] R. Zhou, B. Tu, D. Xia, H. He, Z. Cai, N. Gao, G. Chang, Y. He, High-performance Pt/Ti(3)C(2)T(x) MXene based graphene electrochemical transistor for selective detection of dopamine, Anal. Chim. Acta 1201 (2022) 339653.
- [22] N. Arif, S. Gul, M. Sohail, S. Rizwan, M. Iqbal, Synthesis and characterization of layered Nb2C MXene/ZnS nanocomposites for highly selective electrochemical sensing of dopamine, Ceram. Int. 47 (2021) 2388–2396.
- [23] H. Huang, R. Jiang, Y. Feng, H. Ouyang, N. Zhou, X. Zhang, Y. Wei, Recent development and prospects of surface modification and biomedical applications of MXenes, Nanoscale 12 (2020) 1325–1338.
- [24] J. Zheng, B. Wang, A. Ding, B. Weng, J. Chen, Synthesis of MXene/DNA/Pd/Pt nanocomposite for sensitive detection of dopamine, J. Electroanal. Chem. 816 (2018) 189–194.
- [25] J. Chen, L. Jiang, W. Wang, Z. Shen, S. Liu, X. Li, Y. Wang, Constructing highly porous carbon materials from porous organic polymers for superior CO(2) adsorption and separation, J. Colloid Interface Sci. 609 (2022) 775–784.
- [26] W. He, X. Ye, T. Cui, Flexible electrochemical sensor with graphene and gold nanoparticles to detect dopamine and uric acid, IEEE Sensor. J. 21 (2021) 26556-26565.
- [27] J. Sun, Z. Ma, H. Cai, J. Di, A photoelectrochemical sensor for ultrasensitive dopamine detection based on composites of BiOI and Au-Ag nanoparticles, Colloids Surf. A Physicochem. Eng. Asp. 666 (2023) 131291.
- [28] M. Li, Z. Zhao, W. Zhang, M. Luo, L. Tao, Y. Sun, Z. Xia, Y. Chao, K. Yin, Q. Zhang, L. Gu, W. Yang, Y. Yu, G. Lu, S. Guo, Sub-monolayer YO(x)/MoO(x) on ultrathin Pt nanowires boosts alcohol oxidation electrocatalysis, Adv Mater 33 (2021) 202162
- [29] B.Y. Xia, H.B. Wu, N. Li, Y. Yan, X.W. Lou, X. Wang, One-pot synthesis of Pt-Co alloy nanowire assemblies with tunable composition and enhanced electrocatalytic properties, Angew Chem. Int. Ed. Engl. 54 (2015) 3797–3801.
- [30] S. Sun, G. Zhang, D. Geng, Y. Chen, R. Li, M. Cai, X. Sun, A highly durable platinum nanocatalyst for proton exchange membrane fuel cells: multiarmed starlike nanowire single crystal, Angew Chem. Int. Ed. Engl. 50 (2011) 422–426.
- [31] K. Yin, Y. Chao, F. Lv, L. Tao, W. Zhang, S. Lu, M. Li, Q. Zhang, L. Gu, H. Li, S. Guo, One nanometer PtIr nanowires as high-efficiency bifunctional catalysts for electrosynthesis of ethanol into high value-added multicarbon compound coupled with hydrogen production, J. Am. Chem. Soc. 143 (2021) 10822–10827.
- [32] L. Zhao, Y. Zhang, L.B. Huang, X.Z. Liu, Q.H. Zhang, C. He, Z.Y. Wu, L.J. Zhang, J. Wu, W. Yang, L. Gu, J.S. Hu, L.J. Wan, Cascade anchoring strategy for general mass production of high-loading single-atomic metal-nitrogen catalysts, Nat. Commun. 10 (2019) 1278.
- [33] Y. Zhou, B. Liu, Y. Lei, L. Tang, T. Li, S. Yu, G.J. Zhang, Y.T. Li, Acupuncture needle-based transistor neuroprobe for in vivo monitoring of neurotransmitter, Small 18 (2022) e2204142.
- [34] Y. Xiong, Y. Ma, L. Zou, S. Han, H. Chen, S. Wang, M. Gu, Y. Shen, L. Zhang, Z. Xia, J. Li, H. Yang, N-doping induced tensile-strained Pt nanoparticles ensuring an excellent durability of the oxygen reduction reaction, J. Catal. 382 (2020) 247–255.
- [35] J. Huang, H. Gu, X. Feng, G. Wang, Z. Chen, Copper nanoparticle/N-doped Ti3C2Tx MXene hybrids with enhanced peroxidase-like activity for colorimetric glucose sensing, ACS Appl. Nano Mater. 5 (2022) 15531–15538.
- [36] C. Fu, Y. Sun, C. Huang, F. Wang, N. Li, L. Zhang, S. Ge, J. Yu, Ultrasensitive sandwich-like electrochemical biosensor based on core-shell Pt@CeO(2) as signal tags and double molecular recognition for cerebral dopamine detection, Talanta 223 (2021) 121719.
- [37] W. Meng, H. He, L. Yang, Q. Jiang, B. Yuliarto, Y. Yamauchi, X. Xu, H. Huang, 1D-2D hybridization: nanoarchitectonics for grain boundary-rich platinum nanowires

- coupled with MXene nanosheets as efficient methanol oxidation electrocatalysts, Chem Eng J 450 (2022) 137932.
- [38] H. Wang, J. Cao, Y. Zhou, X. Wang, H. Huang, Y. Liu, M. Shao, Z. Kang, Carbon dots modified Ti3C2Tx-based fibrous supercapacitor with photo-enhanced capacitance, Nano Res. 14 (2021) 3886–3892.
- [39] A. Thadathil, D. Thacharakkal, Y.A. Ismail, P. Periyat, Polyindole-Derived nitrogen-doped graphene quantum dots-based electrochemical sensor for dopamine detection, Biosensors 12 (2022).
- [40] P.P. Chu, Y.M. Zhang, J.J. He, J.H. Chen, J.J. Zhuang, Y.L. Li, X.Z. Ren, P.X. Zhang, L.N. Sun, B.Z. Yu, S.W. Chen, Defective FeO few-atom clusters anchored on nitrogen-doped carbon as efficient oxygen reduction electrocatalysts for highperformance zinc-air batteries, Small Methods 6 (2022) 2200207.
- [41] H. Gu, Y. Xing, P. Xiong, H. Tang, C. Li, S. Chen, R. Zeng, K. Han, G. Shi, Three-dimensional porous Ti3C2Tx MXene–graphene hybrid films for glucose biosensing, ACS Appl. Nano Mater. 2 (2019) 6537–6545.
- [42] H. Huang, Y. Wei, Y. Yang, M. Yan, H. He, Q. Jiang, X. Yang, J. Zhu, Controllable synthesis of grain boundary-enriched Pt nanoworms decorated on graphitic carbon nanosheets for ultrahigh methanol oxidation catalytic activity, J. Energy Chem. 57 (2021) 601–609.
- [43] Q. Li, X. Xu, J. Guo, J.P. Hill, H. Xu, L. Xiang, C. Li, Y. Yamauchi, Y. Mai, Two-dimensional MXene-polymer heterostructure with ordered in-plane mesochannels for high-performance capacitive deionization, Angew. Chem. Int. Ed. 60 (2021) 26528–26534.
- [44] M. Han, J. Yang, J. Jiang, R. Jing, S. Ren, C. Yan, Efficient tuning the electronic structure of N-doped Ti-based MXene to enhance hydrogen evolution reaction, J. Colloid Interface Sci. 582 (2021) 1099–1106.
- [45] N.S. Anuar, W.J. Basirun, M. Shalauddin, S. Akhter, A dopamine electrochemical sensor based on a platinum-silver graphene nanocomposite modified electrode, RSC Adv. 10 (2020) 17336–17344.
- [46] S. Schindler, T. Bechtold, Mechanistic insights into the electrochemical oxidation of dopamine by cyclic voltammetry, J. Electroanal. Chem. 836 (2019) 94–101.
- [47] Z. Zhang, Y. Sun, B. Wang, Y. Ai, F. Shi, Y. Yao, X. Niu, W. Sun, Preparation of AuNPs/MXene nanocomposite for the electrochemical determination of dopamine, Int. J. Electrochem. Sci. 17 (2022) 220561.
- [48] U. Amara, B. Sarfraz, K. Mahmood, M.T. Mehran, N. Muhammad, A. Hayat, M. H. Nawaz, Fabrication of ionic liquid stabilized MXene interface for electrochemical dopamine detection, Mikrochim. Acta 189 (2022) 64.
- [49] J. Paul, J. Kim, Reticular synthesis of a conductive composite derived from metalorganic framework and Mxene for the electrochemical detection of dopamine, Appl. Surf. Sci. 613 (2023) 156103.
- [50] G.S. Arif N, M. Sohail, et al., Synthesis and characterization of layered Nb2C MXene/ZnS nanocomposites for highly selective electrochemical sensing of dopamine, Ceram. Int. 47 (2021) 2388–2396.
- [51] M. Lian, Y. Shi, W. Zhang, J. Zhao, D. Chen, Nitrogen and sulfur co-doped Nb2C-MXene nanosheets for the ultrasensitive electrochemical detection dopamine under acidic conditions in gastric juice, J. Electroanal. Chem. 904 (2022) 115849.
- [52] U. Amara, M.T. Mehran, B. Sarfaraz, K. Mahmood, A. Hayat, M. Nasir, S. Riaz, M. H. Nawaz, Perylene diimide/MXene-modified graphitic pencil electrode-based electrochemical sensor for dopamine detection, Mikrochim. Acta 188 (2021) 230.
- [53] Y. Wang, P. Zhao, B. Gao, M. Yuan, J. Yu, Z. Wang, X. Chen, Self-reduction of bimetallic nanoparticles on flexible MXene-graphene electrodes for simultaneous detection of ascorbic acid, dopamine, and uric acid, Microchem. J. 185 (2023) 108177
- [54] X. Zan, H. Bai, C. Wang, F. Zhao, H. Duan, Graphene paper decorated with a 2D array of dendritic platinum nanoparticles for ultrasensitive electrochemical detection of dopamine secreted by live cells, Chemistry 22 (2016) 5204–5210.